Non-destructive, whole-plant phenotyping reveals dynamic changes in water use efficiency, photosynthetic efficiency, and rhizosphere acidification of sorghum accessions under osmotic stress

Full names and emails:

Daniel N. Ginzburg: dg632@cam.ac.uk[$]

Jack A. Cox: cox.a.jack@gmail.com

Seung Y. Rhee: rheeseu6@msu.edu[#]

Institutional address:

Department of Plant Biology, Carnegie Institution for Science, Stanford, US

[$]Present address: Department of Plant Sciences, University of Cambridge, Cambridge, CB2 3EA, UK

[#]Present address: Plant Resilience Institute, Departments of Biochemistry and Molecular Biology, Plant Biology, and Plant, Soil, and Microbial Sciences, Michigan State University, East Lansing, US

Corresponding authors: Daniel N. Ginzburg and Seung Y. Rhee

Keywords: noninvasive whole-plant phenotyping, modular phenotyping, water use efficiency, *Sorghum bicolor*, osmotic stress, hydroponics

Abstract:

Noninvasive phenotyping can quantify dynamic plant growth processes at higher temporal resolution than destructive phenotyping and can reveal phenomena that would be missed by end-point analysis alone. Additionally, whole-plant phenotyping can identify growth conditions that are optimal for both above- and below-ground tissues. However, noninvasive, whole-plant phenotyping approaches available today are generally expensive, complex, and non-modular. We developed a low-cost and versatile approach to non-invasively measure whole-plant physiology over time by growing plants in isolated hydroponic chambers. We demonstrate the versatility of our approach by measuring whole-plant biomass accumulation, water consumption, and water use efficiency every two days on unstressed and osmotically-stressed sorghum accessions. We identified relationships between root zone acidification and photosynthetic efficiency on whole-plant water use efficiency over time. Our system can be implemented using cheap, basic components, requires no specific technical expertise, and is suitable for any non-aquatic vascular plant species.

Introduction:

Water and nutrient availability, along with the efficiency of their use by crops, are major determinants of agricultural productivity (Fageria et al., 2007; Sinclair and Rufty, 2012). However, unchecked demand for natural resources, such as land, fertilizer, and water, to support global agricultural production has led to widespread ecosystem degradation and biodiversity loss (Foley et al., 2005; Williams et al., 2020). Thus, the demand for stable agricultural yields amidst globally changing climate and decreasing natural resource availability necessitates more resource-efficient and climate-resilient crops and agronomic practices.

Plant growth is neither linear over time (Paine et al., 2011) nor uniform across genotypes within a species (Mortlock and Hammer, 1999; Sugiyama et al., 2012). Measurements taken at single time points thus fail to capture the dynamic variation of plant growth across developmental stages and environmental conditions (Granier and Vile, 2014). In addition to being generally higher throughput than destructive measurements, noninvasive phenotyping approaches provide a window into temporal dynamics along a developmental trajectory and in response to changing environmental conditions. Immense progress has been made in high-throughput phenotyping to capture plant traits non-invasively, particularly through the use of advanced imaging platforms (Shakoor et al., 2017; Li et al., 2020). For example, by non-invasively tracking growth over time in various *Setaria* spp., in which visual leaf area strongly correlates with above-ground biomass, Fahlgren and colleagues uncovered species-specific growth dynamics across time and environmental conditions which would have otherwise been missed by endpoint measurements alone (Fahlgren et al., 2015).

In contrast to phenotyping approaches that capture data from only certain plant parts, whole-plant phenotyping can identify phenotypes and growth conditions that are optimal for both above- and below-ground tissues, and is thus likely more valuable for breeding more resilient and resource-efficient crops (Chochois et al., 2015). Because of the relative difficulty and time required to measure traits at the whole-plant level (Li et al., 2020), measurements are often simplified to include only above-ground plant tissue. However, approaches that exclude root

biomass are potentially limited in value. For example, identifying genetic variation in traits such as biomass accumulation and water use efficiency is particularly important in the context of water-limited conditions in which the ratio of root:shoot biomass is often substantially different than under water-replete conditions (Hubick et al., 1986; Benjamin et al., 2014; Xu et al, 2015). Even in well-watered conditions, the ratio of root:shoot biomass partitioning can be different among genotypes (Chochois et al., 2015; Chenu et al., 2018), further highlighting the importance of including below-ground biomass to accurately quantify resource use efficiency (Leakey et al., 2019).

Various approaches can phenotype below-ground traits non-invasively. For example, root growth can be measured *in vivo* using magnetic resonance imaging (MRI) (Rascher et al., 2011), or with luminescence-based reporters (Rellán-Álvarez et al., 2015). When combined with non-destructive techniques to measure above-ground tissues, such approaches could in theory measure whole-plant growth over time. However, these approaches often require large upfront costs, state-of-the-art technologies, or specific technical expertise (Großkinsky et al., 2015). There are reports of cheaper and simpler approaches to measure whole-plant traits non-destructively (Fletcher et al., 2018). However, the authors found that data obtained non-destructively did not correlate well with values from plants harvested for end-point measurements.

To address the various limitations of measuring whole-plant traits non-destructively, we developed a low-cost and versatile approach that can non-invasively measure whole-plant physiology over time. As a proof of concept, we measured biomass accumulation and water consumption over time to directly quantify whole-plant water use efficiency. Plant water use efficiency (WUE), broadly defined as the ratio of biomass accumulation to water use via transpiration (Vadez et al., 2014), represents an important metric to optimize for improving plant resilience and agricultural sustainability. Various methods exist to quantify WUE, ranging from instantaneous measurements at the leaf-scale (Vadez et al., 2014), to long-term quantification at the canopy scale (Lambers and Oliveira, 2019). Because of the difficulty in measuring whole-plant WUE, it is common to extrapolate these data from leaf-level measurements or via proxies. For example, quantifying leaf gas exchange rates can provide a measure of both photosynthetic and transpiration rates. However, instantaneous leaf-level WUE data are often in disagreement with whole-plant measurements at longer timescales (Medrano et al., 2015). Leaf carbon isotope discrimination (CID) is often used to estimate whole-plant WUE as CID is strongly correlated with WUE in C_3 species (Farquhar et al., 1982). However, the strength of this correlation is greatly reduced in C_4 species, including important crops such as maize or sorghum (Henderson et al., 1998; Vadez et al., 2014). Moreover, quantifying CID is relatively slow and expensive (Vadez et al., 2014), thus necessitating simpler and more widely applicable methods.

In contrast to these methods, our approach, which uses hydroponic cultivation, allows for the direct and non-destructive measurement of whole-plant WUE through direct quantification of biomass accumulation and water use. We show that hydroponic cultivation results in WUE equal to that of soil-grown plants and then demonstrate the temporal and contextual versatility of our approach by measuring whole-plant WUE every two days on unstressed and osmotically-stressed seedlings. In doing so, we identified relationships between root zone acidification and photosynthetic efficiency on whole-plant WUE over time. Our approach can be implemented

using cheap, basic components and requires no specific technical expertise. It can be implemented for any non-aquatic, vascular plant species and can therefore contribute broadly to identifying and engineering superior crop germplasm.

Results:

We developed a simple, cheap, and modular system to grow and phenotype whole-plant traits non-destructively over time. A detailed, step-by-step protocol can be found at protocols.io; dx.doi.org/10.17504/protocols.io.q26g7p6m1gwz/v1. Briefly, a hole is drilled into screw-on caps and a cut-off pipette tip of approximately equal diameter is inserted into the hole of the screw-on cap (Figure 1A). Soil is then inserted into the snugly-fit pipette tips and seeds are sown into the soil-filled tips. Plants are initially grown in “open” hydroponic conditions such that all samples are grown in a single reservoir whose water is exposed to the air (Figure 1B). Upon reaching a desired size, age, or developmental stage, tops are screwed onto tubes and the system becomes “closed” such that water loss from the tube is restricted to uptake by the plant (Figure 1C). By unscrewing the tops, the entire plant can be removed, weighed, and then screwed back onto the tube for continued growth (Figure 1C-D). When grown this way, whole-plant biomass accumulation and water consumption can be assayed repeatedly over time (Figure 2A-B). Moreover, the modularity of our approach allows for precise control of the root environment to investigate a variety of phenotypes, including the relationship of whole-plant biomass accumulation and water consumption in response to changing abiotic or biotic conditions.

As a proof-of-concept of this approach, we sought to compare genotype-specific variation in biomass accumulation, water use, and whole-plant WUE of various sorghum accessions when grown either in soil or using our closed-system hydroponic approach. Sorghum (*Sorghum bicolor*) is a highly productive and relatively stress resistant C_4 crop (Ananda et al., 2020; Khalifa and Eltahir, 2023). It is among the world’s most important cereal crops and is utilized for both food and bioenergy (Ananda et al., 2020; Khalifa and Eltahir, 2023). Genotype-specific variation exists in whole-plant WUE in soil-grown sorghum (Balota et al., 2008; Xin et al., 2008). We selected five sorghum genotypes (Table 1) to represent a diverse range of geographic origins, taxonomic races, variation in transpiration rates measured at the leaf-level (Balota et al., 2008), and variation in WUE measured at the whole-plant level (Balota et al., 2008, Xin et al., 2008).

Table 1: Description of sorghum accessions used in this study

Accession*	Race	Origin**	References
RTx430 (PI 629034)	Caudatum	USA	Miller, 1984; Menz et al., 2004
BTx623 (PI 564163)	Kafir x Caudatum	USA	Menz et al., 2004; Luo et al., 2016
Liang Tang Ai (PI 656046)	Bicolor	China	Xin et al., 2008

Grassl (PI 154844)	Caudatum	Uganda	Boatwright et al., 2021
Tx7078 (PI 656487)	Kafir	USA	Menz et al., 2004; Xin et al., 2008

* Plant introduction (PI) numbers from USDA's Office of Seed and Plant Introduction are included underneath accession names.
** Origin refers to where the accession was bred. However, parental lines may have different origins.

We first asked whether our method of quantifying WUE is consistent with established methods (Cernusak et al., 2006; Xin et al., 2009) by comparing the WUE of plants grown in our hydroponic system to plants grown in soil. Because most traditional soil-grown approaches to directly measure WUE are destructive, we compared end-point biomass accumulation and water use over the course of 8 days after reaching the third leaf stage in either hydroponic or soil-growth conditions. All genotypes accumulated more biomass and consumed more water when grown in soil compared to when grown hydroponically (Figure S2A-B). However, WUE after 8 days was indistinguishable between soil and hydroponic conditions for all genotypes (Figure S2C).

Next, we asked whether evaporative loss of water over time was negligible compared to plant water consumption, which is required to accurately infer plant water use from changes in tube weight over time. Water loss over time due to evaporation was measured in tubes from which plant roots and shoots were cut off to eliminate transpiration. Over the course of seven days, plant-less samples lost an average of 0.6 mL of water due to evaporation (Figure S3), equivalent to approximately 0.7% of average water consumption in plants grown in control conditions over the same period. Evaporative water loss in our hydroponic system was therefore determined to be negligible compared to transpirational water uptake.

Having validated our system, we next sought to compare the effect of osmotic stress on cumulative biomass accumulation, water consumption, and WUE across five sorghum accessions (Table 1). Specifically we asked how these traits vary over time across each accession and whether genotype-specific differences in plant physiology manifest in unstressed or osmotically-stressed conditions. Plants were grown in tubes containing either nutrient solution alone or nutrient solution with 10mM mannitol to induce osmotic stress. Over the course of 8 days in control conditions, biomass accumulation, water consumption, and WUE increased linearly and at an equal rate over time for all genotypes (Figures 2A-C; Table 2). Biomass accumulation and water consumption also increased linearly over time for all genotypes in mannitol-stress conditions, but to a lesser extent than when grown in control conditions (Figure 2A-B). There was a strong linear relationship between biomass accumulation and water consumption for all genotypes in both control and mannitol-treated samples, though this relationship was stronger in control conditions (Figure S4A). Under control conditions, both biomass accumulation and water consumption could in part explain increases in WUE, though biomass accumulation was the stronger predictor of WUE (Figures S4B-C). Under osmotic stress, however, WUE could be explained in part by biomass accumulation only in RTx430, LTA, and Grassl, whereas there was no linear relationship between water use and WUE for any genotype (Figures S4B-C). Unlike under control conditions, genotype-specific differences were

observed in growth and water use trends under mannitol stress. Specifically, Grassl and Tx7078 plants accumulated biomass and consumed water at greater rates than RTx430 plants in mannitol conditions (Table 3). Additionally, in contrast to plants grown in control conditions, WUE of plants grown exposed to mannitol remained constant over time for all genotypes except LTA, in which it gradually decreased over time (Figure 2C; Table 3). These results indicate that Grassl and Tx7078 are more tolerant to osmotic stress than RTx430 and that LTA is less efficient in using water compared to other accessions when osmotically stressed at the third-leaf stage.

Having observed genotype-specific differences in biomass accumulation, water consumption, and WUE rates specifically in osmotically-stressed conditions, we next sought to identify possible mechanisms for this context-specific difference in plant growth and physiology. Osmotic stress can impair photosynthetic performance (Grzesiak et al., 2006; Chen et al., 2011). We therefore asked whether genotype-specific differences in biomass accumulation, water use, and WUE under mannitol stress could be explained by differences in photosynthetic efficiency. Photosystem II quantum efficiency (F_V/F_M) of the third true leaf decreased linearly over time in both control and mannitol samples for all genotypes, though to a greater extent over time in mannitol-treated samples compared to control samples (Figure 3A). When grown under osmotic stress, F_V/F_M of RTx430 and LTA was reduced by Day 4 compared to controls, whereas decreased photosynthetic efficiency compared to control was not evident until Day 6 in BTx623, Grassl, and Tx7078 (Figure 3A). While F_V/F_M of BTx623 plants decreased at a slower rate compared to all other genotypes in both control and mannitol conditions (Table 4), F_V/F_M of Tx7078 plants surprisingly decreased at a greater rate compared to all other genotypes under mannitol stress (Table 4). These results suggest that photosynthetic capacity at the third-leaf stage was not strongly associated with plant growth and water use under osmotic stress, as BTx623 and Tx7078 accumulated biomass at equal rates under osmotic stress despite differences in the effect of osmotic stress on photosynthetic efficiency.

We next asked if there were any differences between the accessions in their root physiology in response to osmotic stress. By exuding a diverse set of compounds from their roots, plants actively modify their root zone to facilitate nutrient uptake and in response to abiotic stress, including mannitol-induced osmotic stress (Marschner et al., 1986; Falhof et al., 2016; Darko et al., 2019). One of the ways in which plants optimize their rhizosphere properties is via soil acidification (Marschner et al., 1986; Ehrenfeld et al., 2005). Growing plants in closed tubes makes it possible to directly and easily measure rhizosphere acidification. We therefore asked whether and when there were any genotype-specific differences in pH change of the nutrient solution after every two days (delta-pH). The pH of nutrient solution with and without mannitol-supplementation was measured before being added to tubes, and the remaining solution in tubes after two days of plant growth was then measured again (Figure 3B, Table 5, Supplemental File 1). Any solution remaining in the tubes after every 2 days was then discarded and fresh nutrient solution was added to ensure sufficient water for plant growth for the subsequent two days. There were no genotype-specific differences in delta-pH, nor was there an interaction between genotype and time on delta-pH in either control or mannitol-treated samples (2-way analysis of variance (ANOVA); Table S1). However, delta-pH of samples did vary over time in both conditions (Table S1). We therefore asked whether the magnitude of root zone acidification over time varied by growth condition and found that delta-pH changed over

time in a treatment-specific manner (Table 5). After 2 days of measurement, both control and mannitol-treated samples acidified their root zones equally (Figure 3B, Table 5). However, after 4, 6, and 8 days of growth in closed hydroponic conditions, root zone acidification decreased in control samples but was maintained in mannitol-treated samples (Figure 3B, Table 5). These results suggest that prolonged root zone acidification is an adaptive response conserved among sorghum accessions in response to osmotic stress at the seedling stage.

We have demonstrated how non-destructive, whole-plant phenotyping can be employed using simple and readily available components. We showcase the versatility of our approach by directly measuring multiple traits across a diverse set of sorghum accessions in unstressed and osmotically-stressed conditions. Collectively, we illustrate how this method can identify genotype-specific temporal dynamics in plant growth across multiple organs and physiological processes.

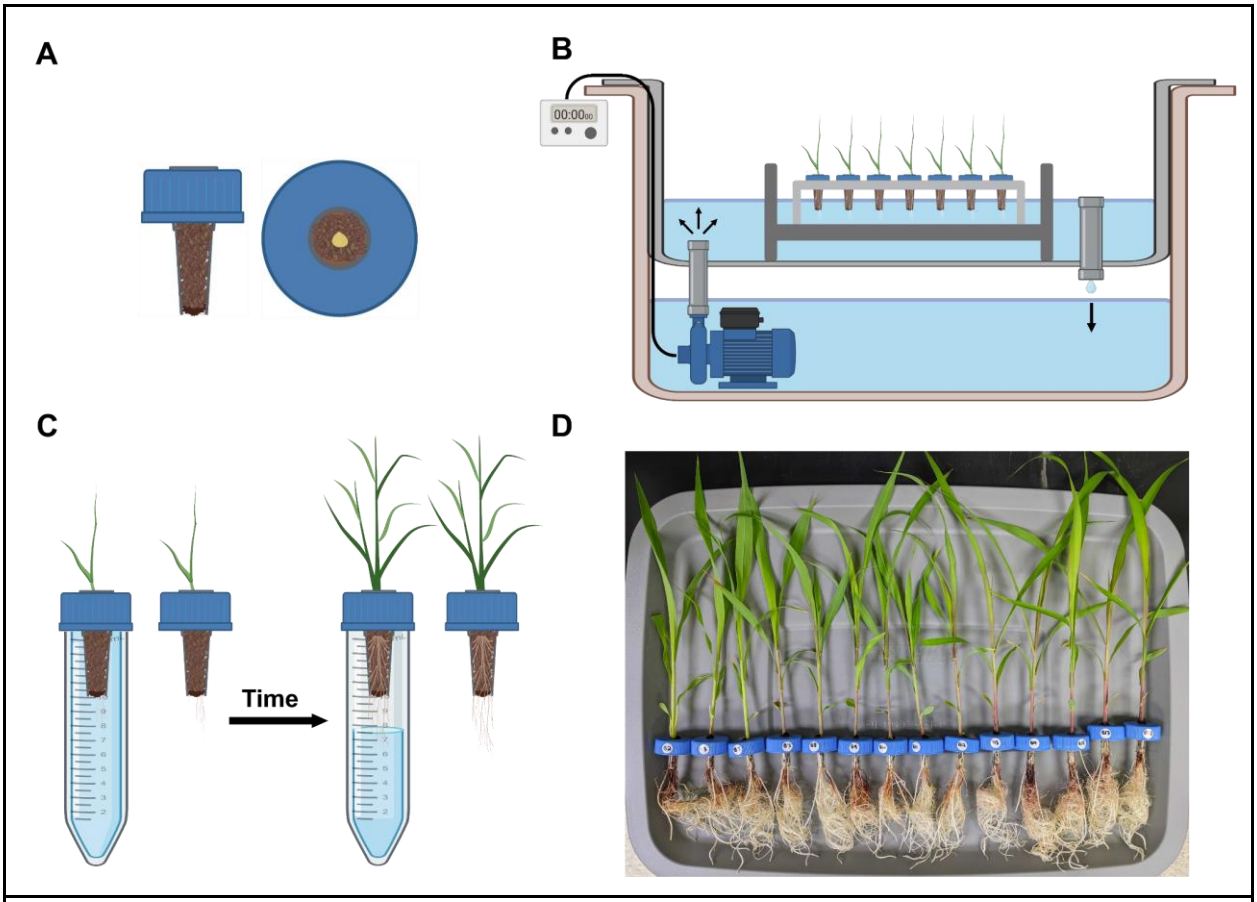

Figure 1: (A) Representation of a screw-on cap with a hole drilled into the top and a cut-off pipette tip inserted into the hole. Soil is inserted into the pipette tips and seeds are sown into the soil-filled tips. (B) Schematic of the recirculating ebb and flow hydroponic system used in this study. Water is pumped up from the bottom reservoir up to the top reservoir, where it rises up to the point of the drain pipe, and then falls back down into the bottom reservoir. Plants are placed in the top reservoir such that the water level rises up to the point of the soil-filled tips. The duration and time of day of irrigation events are controlled via a programmable timer connected to the pump. Samples are grown in these “open” hydroponic conditions until they

reach a predetermined age or developmental stage. (C) Samples are then screwed onto tubes filled with nutrient solution, at which point the system is “closed”. When closed, water loss due to evaporation is prevented. After a designated amount of time, caps are unscrewed and the plants are lifted out of the tube. Tubes and caps with plants can be weighed to determine water consumption and biomass accumulation relative to previous timepoints, respectively. Caps with plants can then be screwed back onto tubes for continued growth in “closed” conditions. (D) Sorghum samples after 8 days of growth in tubes. Graphics for cartoon schematics in A-C are from BioRender.

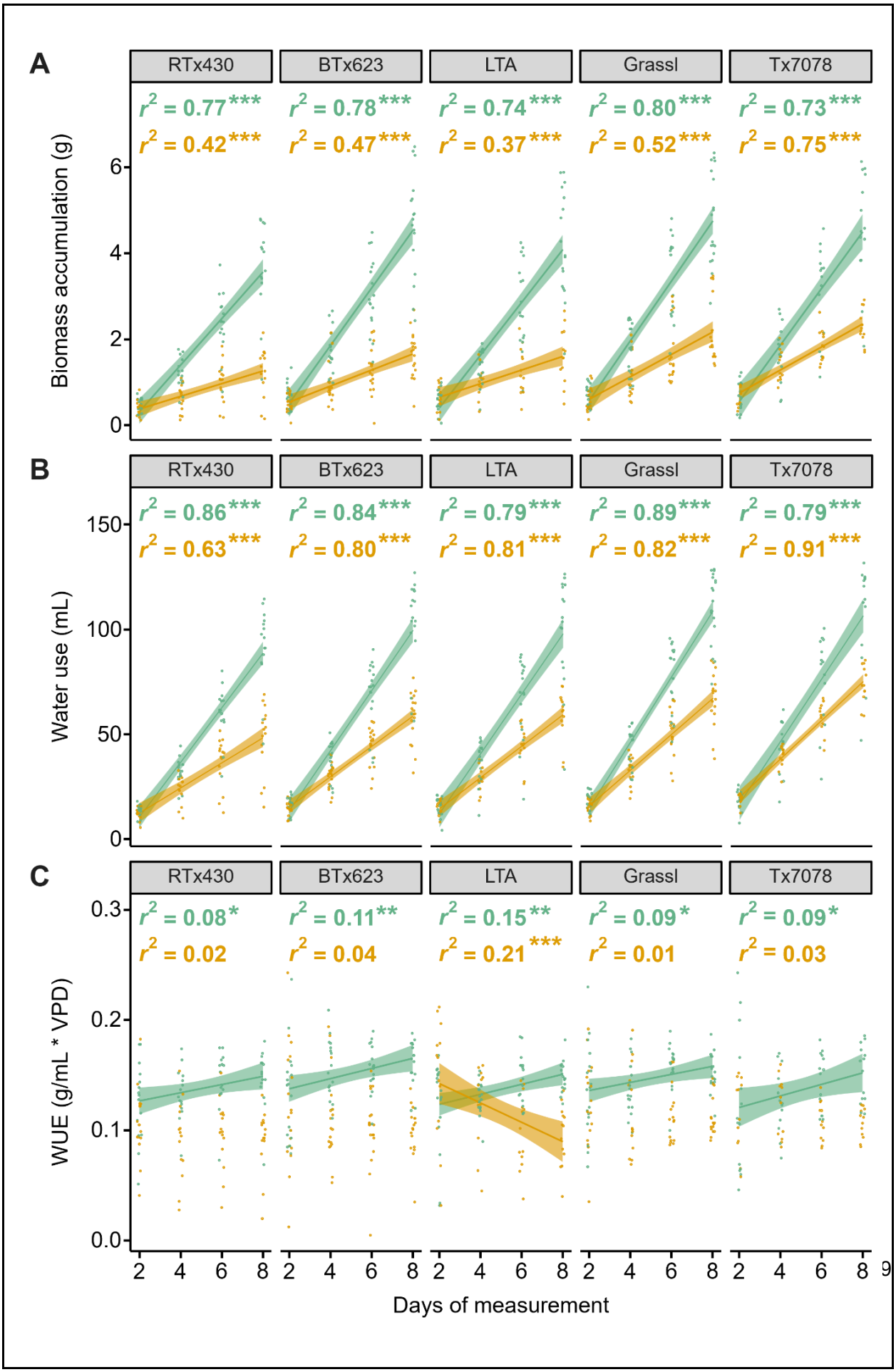
A
RTx430
BTx623
LTA
Grassl
Tx7078
r^2 = 0.77***
r^2 = 0.42***
r^2 = 0.78***
r^2 = 0.47***
r^2 = 0.74***
r^2 = 0.37***
r^2 = 0.80***
r^2 = 0.52***
r^2 = 0.73***
r^2 = 0.75***
Biomass accumulation (g)
0
2
4
6
B
r^2 = 0.86***
r^2 = 0.63***
r^2 = 0.84***
r^2 = 0.80***
r^2 = 0.79***
r^2 = 0.81***
r^2 = 0.89***
r^2 = 0.82***
r^2 = 0.79***
r^2 = 0.91***
Water use (mL)
0
50
100
150
C
r^2 = 0.08*
r^2 = 0.02
r^2 = 0.11**
r^2 = 0.04
r^2 = 0.15**
r^2 = 0.21***
r^2 = 0.09*
r^2 = 0.01
r^2 = 0.09*
r^2 = 0.03
WUE (g/mL * VPD)
0.0
0.1
0.2
0.3
2
4
6
8
Days of measurement

Figure 2: Cumulative biomass accumulation (A), water consumption (B), and WUE (C) of all genotypes over time in control (green) or mannitol-treated (orange) conditions. Solid lines represent the linear regression bounded by the 95% confidence interval (n = 12-18 per genotype, condition, and day; N = 4). r^2 values represent the square of the Pearson correlation coefficient of the linear regression. Asterisks indicate whether the linear relationship is statistically significant: * (p-value < 0.05), ** (p-value < 0.01), *** (p-value < 0.001). Absence of a regression line indicates a non-significant linear relationship. n, number of biological replicates per genotype and condition; N, number of independent experiments.

Table 2: Rate of biomass accumulation, water use, and WUE over time in control conditions

Genotype	Biomass accumulation (g/day)		Water use (mL/day)		WUE [(mg/mL * VPD)/day]	
RTx430	0.54 ± 0.09	A	13.1 ± 1.7	A	3.73 ± 3.35	A
BTx623	0.67 ± 0.09	A	14.3 ± 1.6	A	4.60 ± 3.16	A
LTA	0.61 ± 0.09	A	14.3 ± 1.6	A	4.58 ± 3.16	A
Grassl	0.70 ± 0.08	A	15.6 ± 1.5	A	3.65 ± 3.06	A
Tx7078	0.66 ± 0.09	A	14.9 ± 1.7	A	5.21 ± 3.47	A

Values represent the slope of the linear regression followed by the 95% confidence interval (n = 55-72 per genotype; N = 4). Genotypes which share the same letter are not statistically different as determined by 2-way ANOVA followed by Tukey's HSD (alpha = 0.05). n, number of biological replicates per genotype and condition; N, number of independent experiments.

Table 3: Rate of biomass accumulation, water use, and WUE over time in mannitol conditions

Genotype	Biomass accumulation (g/day)		Water use (mL/day)		WUE [(mg/mL * VPD)/day]	
RTx430	0.15 ± 0.05	A	5.98 ± 0.99	A	no change	-
BTx623	0.19 ± 0.05	AB	7.21 ± 0.90	AB	no change	-
LTA	0.16 ± 0.06	AB	7.46 ± 1.06	AB	-8.80 ± 4.14	-
Grassl	0.26 ± 0.05	B	8.54 ± 0.93	B	no change	-
Tx7078	0.27 ± 0.06	B	9.19 ± 1.10	B	no change	-

Values represent the slope of the linear regression followed by the 95% confidence interval (n = 48-72 per genotype; N = 4). Genotypes which share the same letter are not statistically different as determined by 2-way ANOVA followed by Tukey's HSD (alpha = 0.05). No change indicates a non-significant linear regression. n, number of biological replicates per genotype and condition; N, number of independent experiments.

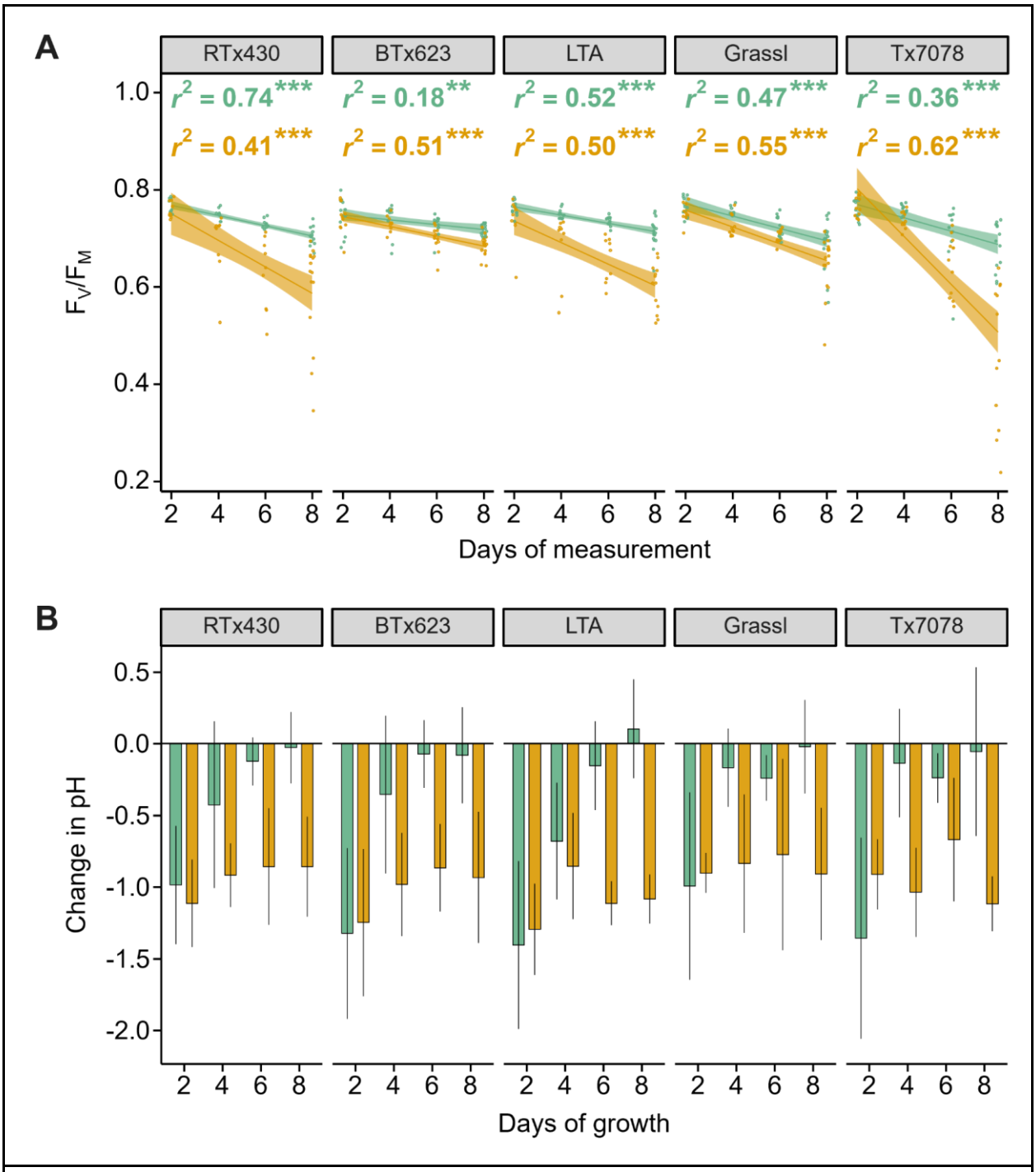

Figure 3: (A) F_V/F_M over time of the third true leaf of samples grown in control (green) or mannitol (orange) conditions. Solid lines represent the linear regression bounded by the 95% confidence interval (n = 9-18 per genotype, condition, and day; N = 3-4). r^2 values represent the square of the Pearson correlation coefficient of the linear regression. Asterisks indicate whether the linear relationship is statistically significant: ** (p-value < 0.01), *** (p-value < 0.001). (B) Bars represent the two-day change in pH of nutrient solution of plants grown in control (green) and mannitol (orange) conditions. Error bars represent the standard deviation (n = 7-18 per genotype, condition, and day; N = 3-4). n, number of biological replicates per

genotype and condition; N, number of independent experiments.

Table 4: Change in F_V/F_M over time

Genotype	Control		Mannitol	
RTx430	-0.010 ± 0.004	AB	-0.027 ± 0.008	b
BTx623	-0.005 ± 0.003	A	-0.010 ± 0.007	a
LTA	-0.008 ± 0.003	AB	-0.022 ± 0.008	ab
Grassl	-0.013 ± 0.003	B	-0.017 ± 0.007	ab
Tx7078	-0.014 ± 0.004	B	-0.049 ± 0.008	c

Values represent the slope of the linear regression followed by the 95% confidence interval (n = 40-54 per genotype and condition; N = 3-4). Genotypes which share the same letter are not statistically different as determined by 2-way ANOVA followed by Tukey's HSD (alpha = 0.05). n, number of biological replicates per genotype and condition; N, number of independent experiments.

Table 5: The effect of treatment and time on 2-day change in pH

Treatment	Days of growth	Average initial pH	Average final pH	Average 2-day change in pH	
Control	2	6.59 ± 0.15	5.37 ± 0.54	-1.22 ± 0.61	A
	4	6.59 ± 0.09	6.24 ± 0.47	-0.35 ± 0.47	C
	6	6.65 ± 0.07	6.49 ± 0.20	-0.16 ± 0.22	CD
	8	6.56 ± 0.09	6.54 ± 0.37	-0.02 ± 0.38	D
Mannitol	2	6.61 ± 0.23	5.52 ± 0.45	-1.09 ± 0.36	AB
	4	6.63 ± 0.11	5.70 ± 0.39	-0.93 ± 0.36	B
	6	6.67 ± 0.06	5.83 ± 0.43	-0.84 ± 0.44	B

	8	6.58 ± 0.10	5.61 ± 0.35	-0.97 ± 0.37	B

Values represent the average initial, final, and 2-day change in pH followed by the standard deviation (n = 43-75 per condition and day; N = 3-4). Days which share the same letter are not statistically different as determined by 2-way ANOVA followed by Tukey's HSD (alpha = 0.05). n, number of biological replicates per genotype and condition; N, number of independent experiments.

Discussion:

Plant phenotypes are dynamic manifestations of genetics, environmental conditions, and developmental stage. Phenotypic plasticity is evidenced by changes in growth of both above- and below-ground tissues. Non-destructive, whole-plant phenotyping facilitates quantification of dynamic growth processes which are more challenging to identify via destructive approaches and is therefore crucial for improving our understanding of plant growth and for engineering more resilient and resource-efficient crops. However, noninvasive, whole-plant phenotyping approaches are often expensive and technically complex. To address these limitations, we developed a cost-effective, simple, and modular approach that can measure whole-plant physiology over time. Unlike soil-grown conditions, hydroponic cultivation allows us to physically isolate roots and return them to their growth environment non-destructively. In doing so, entire plant biomass can be measured directly and repeatedly. Additionally, if each plant is grown physically separated from other plants and evaporation is prevented, plant water use can also be measured directly. These capabilities alone are of practical value for the study of plant growth and development given that these traits are not readily quantifiable in a direct, non-destructive manner for soil-grown plants. Moreover, quantification of these traits over time allows for direct measurements of whole-plant WUE over time. Previous studies have demonstrated creative approaches to quantify WUE non-destructively (Fahlgren et al., 2015; Fletcher et al., 2018). However, these methods either ignore root biomass contributions (Fahlgren et al., 2015), or do not correlate well with WUE values from harvested soil-grown plants (Fletcher et al., 2018).

Comparing our hydroponic system to potted soil, we observed that plant growth and resource usage were strongly influenced by abiotic conditions. This was made clear by the much greater biomass accumulation and water consumption of soil-grown plants compared to those grown hydroponically. Interestingly, WUE was uniform across growth conditions. This suggests that biomass accumulation at this stage of development necessitates a proportionally equal amount of water consumption, regardless of absolute growth rates. What might explain slower growth rates in the hydroponic system compared to potted soil? The hydroponic growth conditions used in this study were chosen to be suitable for a diverse range of genotypes at a specific developmental stage, rather than being designed to optimize growth. However, irrigation scheduling, nutrient composition, and abiotic conditions for hydroponic growth could all be refined to optimize a given metric, as desired.

We chose to examine the five varieties of sorghum (Table 1) because previously genotype-specific differences in whole-plant WUE have been observed in soil-grown sorghum (Mortlock and Hammer, 1999; Xin et al., 2008; Xin et al., 2009). We specifically focussed on

identifying genotype-specific variation at the seedling stage as sorghum biomass accumulation at the time of harvest is most affected by drought-induced osmotic stress when stress occurs at the seedling stage (Mastrorilli et al., 1999), similar to the heightened sensitivity of many crop species to stresses at early stages in their development such as maize (Kang et al., 2000; Ge et al., 2012), rice (Zhao et al., 2014), and tomato (Sivakumar et al., 2020). Previously, LTA exhibited greater whole-plant WUE than Tx7078 when grown in soil, but equal WUE to BTx623 and RTx430 (Xin et al., 2008; Xin et al., 2009). That we did not observe genotype-specific differences in WUE in either soil- or hydroponically-grown sorghum in control conditions could reflect the different ages and developmental stages of the plants being assayed. We measured plant growth starting at the third leaf stage, corresponding to plants which were approximately 2-weeks old, whereas plants were approximately 4-6 weeks old (corresponding to the 8th-leaf stage) in Xin et al., 2008 and Xin et al., 2009. The differences in WUE we observed compared to previous reports further support the idea that WUE varies by developmental stage (Fahlgren et al., 2015). We did, however, observe genotype-specific differences in WUE when plants were grown under osmotic stress. In light of the previously-identified superiority of LTA in terms of its WUE when grown in soil, it was surprising that this was the only genotype tested in this study in which WUE decreased over time when exposed to mannitol. While WUE of many species, including sorghum (Xie and Su, 2012), increases in response to drought stress in soil-grown conditions (Peters et al., 2018), mannitol-induced osmotic stress decreases WUE in multiple species (Cha-Um and Kirdmanee, 2008; Darko et al., 2019), similar to what we observed with sorghum, and thus its effects on plant growth should be viewed as distinct from natural drought-induced stress. Collectively, these findings highlight the importance of considering multiple developmental stages and abiotic conditions when assaying for superior germplasm.

Plant growth is not always linear over time, but rather changes as development progresses and in response to changing environmental conditions, as was shown in Setaria (Fahlgren et al., 2015). Thus, while we observed linear relationships of biomass accumulation and water consumption with time for all genotypes in both control and osmotically-stressed conditions, the rates of these processes likely change over the lifespan of the plant, especially at developmental transitions (Hanley et al., 2004; Borrás et al., 2007). Interestingly, biomass accumulation, rather than reduced water consumption, was a stronger predictor of WUE in control conditions (Figures S4B-C), which has previously been observed in sorghum (Xin et al., 2009). Under osmotic stress, WUE could only be explained in part by biomass accumulation in some genotypes, suggesting that this relationship is underpinned by both genotypic and environmental factors.

The ability to track plant growth over time non-destructively can reveal biological insights that could be missed through endpoint analysis alone (Fahlgren et al., 2015). For example, cumulative WUE of mannitol-treated BTx623 and Tx7078 plants was already lower than control plants by Day 4, yet F_V/F_M in those genotypes was indistinguishable in response to mannitol stress compared to control, suggesting that WUE in sorghum is negatively affected by osmotic stress before photosynthetic capacity changes. However, because biomass accumulation was already reduced by Day 4 in mannitol-treated BTx623 and Tx7078 plants compared to control, something other than a reduction in photosynthetic efficiency was impairing growth rates in those genotypes. End-point analysis would not have revealed how osmotic stress impacted growth and photosynthetic efficiency differently and at different times among the genotypes.

These observations further support the value of non-destructive approaches to capturing the dynamic nature of plant phenotypes across time and environments (Granier and Vile, 2014).

Plants actively modify the soil properties of their growing environment to optimize growth by improving nutrient uptake and mobilization and to regulate soil microbial dynamics (Marschner et al., 1986; Shen et al., 2013; Falhof et al., 2016). Depending on the biotic and abiotic conditions in the soil, roots can exude sugars, amino acids, enzymes, organic acids, and phytosiderophores to optimize conditions for symbiotic rhizospheric microorganisms (Ryan et al., 2009) or for direct nutrient uptake (Marschner et al., 1986; Shen et al., 2013). The non-destructive nature of our closed-system hydroponic approach allowed us to more readily identify a connection between root-zone acidification and biomass accumulation than had we grown plants in soil for destructive end-point analyses. For example, after 2 days of growth in closed tubes, both control and mannitol-treated plants of all genotypes acidified their root zones equally. At this time point, there was also no difference in total biomass accumulation or water consumption between control and mannitol-treated samples in any genotype. After Day 2, though, root zone acidification continued in mannitol-treated plants but not in control samples. In addition, we observed greater biomass accumulation and water consumption in control plants relative to mannitol-treated samples from that point onwards. That mannitol-treated plants continued to acidify their root zone at levels equal to that of Day 2 suggests a greater and prolonged investment of root exudates to actively modify their root environment. This could be because mannitol-stress can impair uptake and translocation of phosphorus (Resnik, 1970) and potassium (Slama et al., 2007). Interestingly, the average pH after every two days of growth in mannitol was 5.5-5.8 (Table 5), which is a range that favors plant uptake of all essential nutrients (Bailey, 1996; Pennisi and Thomas, 2009). Thus, root zone acidification in response to mannitol stress could be an adaptive response to improve mineral nutrient uptake and mobility.

Various aspects of the dynamic effects of root-zone conditions on plant growth remain poorly understood (Kardol et al., 2013). Additionally, many plant responses to environmental conditions are age-dependent (Bond, 2000; Panter and Jones, 2002). Thus, while hydroponic cultivation is an established approach in plant biology research (Asao, 2012), the isolation and modularity of the root zone environment afforded by our approach open the door to additional avenues of experimentation for directly studying dynamic, and age-dependent processes. For example, researchers could finely control the characteristics of the solution in each tube to investigate temporal effects of mineral nutrition or biotic stress on whole-plant development and physiology and to analyze how these characteristics differentially affect shoot vs. root growth. Our approach also makes it easier to investigate how changes in root architecture and morphology over time influence plant growth. Some plant species require more oxygen in their root zone than others (Narsai et al., 2011; Asao, 2012). Species that require greater levels of root zone oxygenation than sorghum could be supplemented with hydrogen peroxide to improve the availability of dissolved oxygen in the growing media (Butcher et al., 2017; Liu et al., 2022). While suitable concentrations of hydrogen peroxide would need to be established beforehand, its use in the nutrient solution would not require any physical modifications to the closed-hydroponic design. Additionally, tubes could be opened daily, rather than every two days, to further increase root zone oxygenation.

Efforts to identify and engineer more resource-efficient and resilient crops will benefit from phenotyping approaches which can noninvasively quantify whole-plant growth and

physiology over time. Our approach allows for inherently greater throughput than traditional approaches and can, in its entirety, be implemented using cheap and readily available components. Its versatility for studying various aspects of plant growth and physiology make it a valuable method for plant scientists as a whole in studying plant growth and for identifying superior and more resilient crops.

Materials and Methods

A detailed, step-by-step protocol can be found at protocols.io; dx.doi.org/10.17504/protocols.io.q26g7p6m1gwz/v1.

Closed-system hydroponic growth apparatus construction and seeding

Screw-on tops of 50mL Falcon tubes were used to both physically support growing plants and to secure individual tubes to prevent evaporative water loss. To physically support growing plants, holes were drilled into the center of 50mL Falcon tube caps using a 21/64 inch drill bit. 1250 uL pipette tips were cut ~3 cm from the tip (narrower) end and inserted into the pre-drilled Falcon tube caps such that the tips fit snugly into the holes in the caps and rested almost flush with the top of the cap. Rapid-Rooter starter plugs (General Hydroponics, Santa Rosa, CA, USA) were cut into rectangular slices of ~0.5cm length and ~0.9cm width and were inserted into the top of each tip and then gently pushed to the bottom. To prevent unnatural water retention and pressure buildup in the filled tips, pinholes were created in the tips ~25% from the bottom using a needle. Caps with tips were then filled with fresh Pro Mix Bio-Fungicide potting soil (Premier Tech Horticulture, Quakertown, PA, USA), placed in tube racks, and left to soak overnight in tap water which reached the bottom of the tops but did not submerse the caps. The next day, individual sorghum seeds were planted into soil-filled tips. While still in racks, all samples were then placed into an in-house built ebb & flow (flood & drain) hydroponic system.

Briefly, an ebb & flow system utilizes a submersible pump to recirculate nutrient-rich water between two or more reservoirs. Plants are placed within one of the reservoirs and grown hydroponically. The ebb & flow system used in this study consisted of two, 18 gallon Rubbermaid Roughneck plastic totes (reservoirs) (Rubbermaid, Atlanta, GA, USA), one stacked on top of the other (Figure S1A). Two, ¾ inch diameter holes were drilled in opposite corners of the top reservoir. A ¾ inch threaded and barbed bulkhead fitting (Figure S1B) (Botanicare, Vancouver, WA, USA) was inserted from above into one of the drilled holes and fastened from below with a rubber washer. Water in an ebb and flow system needs to reach, but not submerge, the seedlings in the upper reservoir. Thus, to increase the irrigation height the water reaches in the upper reservoir before draining back down, a threaded height extender (Figure S1B) was then screwed into this first hole from above. The second hole which was drilled into the upper reservoir was then fitted with a threaded, plastic debris screen (Figure S1B) to allow water to gently pump up into the top reservoir. In the bottom reservoir sat an 8W, 800 liter/hour submersible pump (VIVOSUN, Ontario, CA, USA) connected via PVC plastic tubing to the barbed end of the bulkhead fitting (Figure S1A). When turned on, water is pumped up to the top reservoir from below and rises up to the level of extender before draining back down to the bottom reservoir. In order for water to constantly recirculate during irrigation, sufficient water must be added to the ebb & flow system to allow for filling the top reservoir up to the draining height and to ensure enough water is in the bottom reservoir to be pumped back up. To control the duration and number of irrigation events each day, the pump was connected to a digital programmable timer (BN-LINK, Santa Fe Springs, CA, USA).

Pre-phenotyping hydroponic growth conditions

The drainage height of the ebb & flow system was optimized such that, during irrigation, the bottom ~2-3cm of the cut pipette tips would be submerged in water (Figure 1B). Before seedling emergence, samples were irrigated thrice daily with tap water for 5 minutes every 8 hours using a programmable timer as described above. Upon root emergence (root tips growing below the bottom of the pipette tip) of 50% of the samples, seedlings were irrigated every hour with a single, 15-minute irrigation event using a programmable timer. At this point, Peters Professional General Purpose 20-20-20 soluble fertilizer (ICL Specialty Fertilizers, Tel Aviv, Israel) was directly added to the lower water reservoir using a 50mL plastic scoop up to an electrical conductivity (EC) of 1200 mS/cm (~1.25g fertilizer/liter water) while the water was being circulated. EC was measured with a Hanna Edge conductivity meter (Hanna Instruments, Rhode Island, USA). Upon root emergence of all samples, irrigation duration was increased to 45-minute events every hour followed by 15 minutes of no irrigation to increase root zone oxygenation. The reservoir was emptied and refilled with fresh nutrient solution every 3-4 days. All experiments were conducted in a greenhouse with supplemental lighting from high pressure sodium lamps from 7am-7pm daily.

Transitioning samples from open- to closed-hydroponic conditions

Once 50% of samples reached the 3rd true-leaf stage, a bulk nutrient solution was prepared such that 40mL of solution could be allocated to each sample in 50mL Falcon tubes. Nutrient solution in 50mL tubes consisted of 0.4g/L Hoagland's No. 2 basal salt mixture (Sigma Aldrich Chemical Co. St. Louis, MO, USA) supplemented with ~0.5g/L Professional General Purpose 20-20-20 fertilizer up to an EC of 1200 mS/cm. This bulk nutrient solution was then split into two, and mannitol was added into one of the solutions up to a concentration of 10mM. pH of both control and mannitol-supplemented solutions was then recorded. 50 mL tubes were then filled with 40mL of either control or mannitol-supplemented nutrient solution. Tubes were wrapped in aluminum foil to prevent algal growth. Tubes with solution, but no caps, were then weighed. Caps containing seedlings were then brought into the lab and were firmly screwed onto individual tubes. Tubes with seedlings screwed on were then weighed to determine initial seedling weight. If the roots of any sample did not reach the nutrient solution when fully closed into the cap, additional solution was added and the tube (with and without cap) was reweighed. Samples were evenly spaced into 50mL tube racks then returned to the greenhouse.

Quantifying biomass accumulation, water use, and change in media pH

Every two days, fresh nutrient solution was prepared and pH was measured as described above for both control and 10mM-treated samples. Seedlings and caps were unscrewed from their tubes and placed back into the ebb & flow system (operating with constant irrigation) to keep the roots hydrated while tubes were weighed. 50mL tube caps (without holes) were screwed onto each tube to prevent evaporation. Tubes were brought back into the lab and were individually weighed (without caps). pH of the solution in each tube was also recorded at this time. Tubes were emptied of their solution and refilled with new control or 10mM mannitol-supplemented solution up to 40mL as described above. Tubes without caps were then weighed again and caps were screwed back on to prevent evaporation. Seedlings were brought into the lab, individually weighed, and then screwed back onto their corresponding tubes before being returned to the greenhouse.

Chlorophyll fluorescence quantification

In the greenhouse, seedlings were gently laid on their side and dark-adaptation clips were placed onto the middle of the 3rd true leaf of each sample for 30 minutes. After dark-adaptation, F_V/F_M of the 3rd true leaf was recorded using a chlorophyll fluorometer (OS30p+, Opti-Sciences, Inc. Hudson, New Hampshire). Specifically, minimum fluorescence (F_0) was measured after application of a weak modulated pulse of 0.1 µmol m^{-2} s^{-1} PPFD to the sampled region. A 1-second saturating pulse of 6,000 µmol m^{-2} s^{-1} PPFD was subsequently applied to the same region to determine maximum fluorescence (F_M). F_V/F_M was calculated as $(F_M-F_0)/F_M$. F_V/F_M measurements were always made between 2-3pm, as chlorophyll fluorescence parameters are under circadian regulation (Dodd et al., 2014). Samples were then placed upright back into tube racks.

Determination of vapor pressure deficit

In addition to genetic and developmental factors, plant transpiration rates are driven by vapor pressure deficit (VPD) (Mortlock and Hammer, 1999; Vadez et al., 2014; Grossiord et al., 2020), which is the difference between ambient vapor pressure and vapor pressure in saturated air (Grossiord et al., 2020). To facilitate comparisons of WUE across time and experiments, we therefore normalized WUE at each timepoint by the average cumulative daytime VPD (Sinclair, 2012; Vadez et al., 2014). Temperature and humidity were measured continuously with a Govee H5075 thermometer-hygrometer (Govee Moments Trading Limited, Hong Kong) and were averaged over 15-minute intervals. VPD was derived from temperature and RH values using the following equations from Murray (1967):

1. Saturation vapor pressure (SVP) in kPA = $0.61078 * e^{(T / (T + 237.3) \times 17.2694)}$ where T is temperature in degrees Celsius
2. Actual vapor pressure $(\mathrm{AVP}) = (\mathrm{SVP} * \mathrm{RH}) \div 100$ where RH is percent relative humidity
3. VPD = SVP - AVP

Daytime VPD was calculated as the average VPD during the hours when supplemental lighting was provided in the greenhouse, namely 7am-7pm.

Determination of evaporative loss in closed-hydroponic system:

Plants were grown hydroponically in soil-filled pipette tips as described above. At the 3rd leaf stage, roots and shoots were cut from the bottom of the tips and the base of the cap, respectively to prevent plant water uptake. An equal number of tubes as caps were filled with 1200 EC nutrient solution and weighed, as described above. Caps from which roots and shoots were cut off were then screwed onto nutrient-filled tubes. Samples were placed in the same greenhouse as described above. Over the course of seven days, caps were removed from tubes and tubes were weighed to determine average daily and cumulative water loss due to evaporation. Caps were then screwed back on after weighing. This experiment was repeated three times.

Average 7-day water consumption on control plants was derived from the linear regression model of water use as a function of time. Cumulative water loss of plant-less samples was then divided by the computed 7-day plant water use to represent the percentage of plant water use.

Determination of water use efficiency from soil-grown plants:

Seeds were planted in pots filled with an equal amount, by weight, of Pro Mix Bio-Fungicide potting soil. Soil-grown plants were grown in the same greenhouse as hydroponically-grown plants, as described above. When 50% of the samples reached the 3rd true leaf stage, at least three samples per genotype were harvested to determine average total biomass per genotype (initial biomass). Samples harvested at the 3rd true leaf stage were visually of similar size to those which were not yet harvested. For the remaining samples, pots were watered up to the point of soil saturation and were then weighed. The soil surface and drainage holes at the bottom of each pot were then covered with aluminum foil to prevent evaporative water loss. After 8 days of growth, the aluminum foil was removed and pots with plants were weighed. Plants were then harvested to determine final, whole-plant biomass. Eight-day biomass accumulation was calculated as (final biomass - initial biomass). Water consumption was calculated as (initial pot weight - average initial biomass) - (final pot weight - final whole-plant biomass). Soil-grown WUE was normalized by average cumulative daytime VPD, as described above.

Statistical Analyses:

All statistical analyses were performed using functions from the ‘lsmeans’ package (Lenth, 2016) in R version 4.2.2. Linear regressions and their statistical comparisons were calculated using the lm() and lstrends() functions, respectively. Differences in delta-pH were calculated by two-way ANOVA followed by Tukey’s HSD test (p-value < 0.05) using the lsmeans() function. Comparisons of biomass accumulation, water use, and WUE between soil- and hydroponically-grown samples were calculated by two-way ANOVA followed by Tukey’s HSD test (p-value < 0.05) using the lsmeans() function.

Supplemental Figures:

Figure S1: Images of Botanicare fittings used in the ebb and flow system. (A) threaded bulkhead fitting which is inserted into both holes that are drilled into the upper reservoir; (B) threaded plastic debris screen; (C) threaded height extender; (D) debris screen screwed onto bulkhead fitting for water inflow into the upper reservoir; (E) debris screen screwed onto two height extenders for water flowing out of the upper reservoir and back down into the lower reservoir. Images of Botanicare fittings are from https://www.hawthornegc.com.

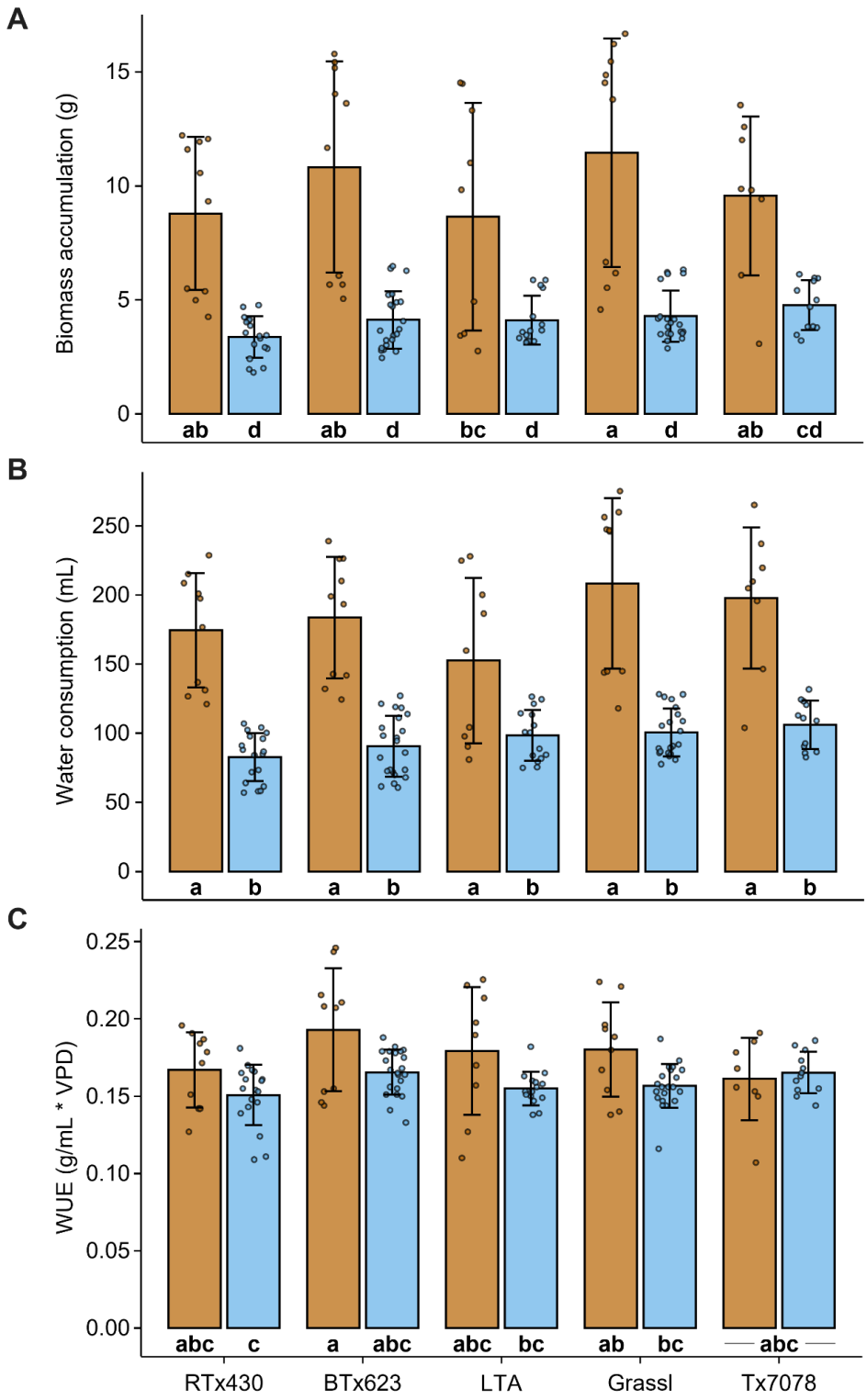

Figure S2: (A) Biomass accumulation, (B) water use, and (C) WUE of plants grown in soil (brown) or hydroponically (blue). Error bars represent the standard deviation (n = 8-22; N = 3-4). Letters represent significantly different groups as determined by two-way ANOVA followed

by Tukey's HSD test (alpha = 0.05). n, number of biological replicates per genotype and condition; N, number of independent experiments.

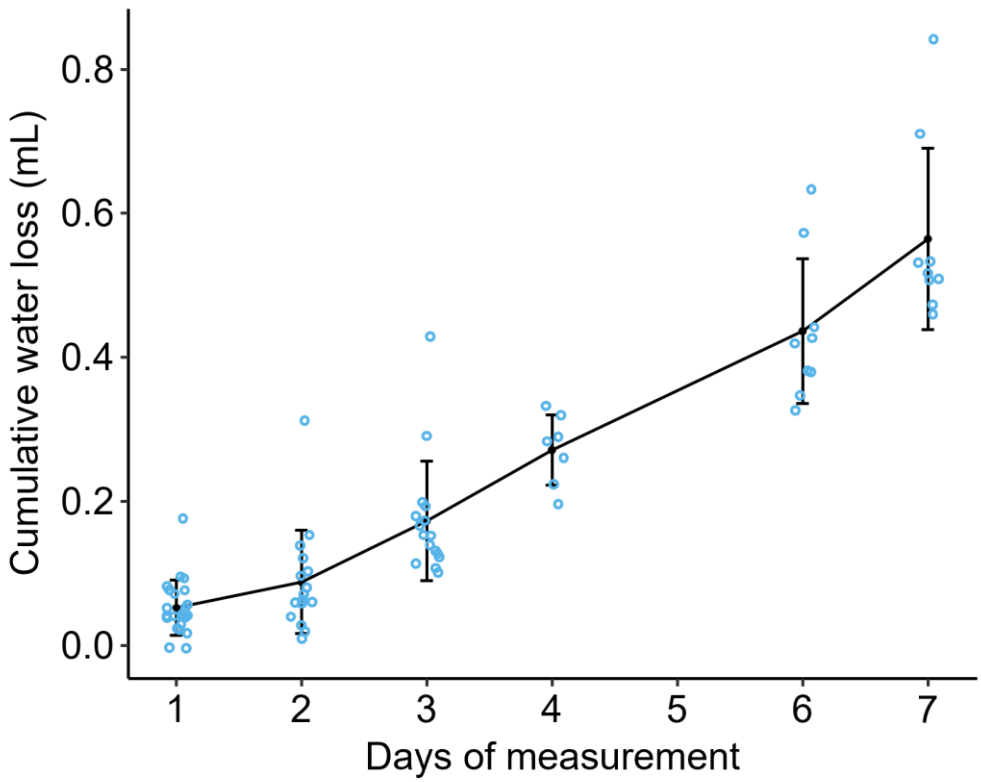

Figure S3: Water loss due to evaporation in closed hydroponic tubes. Black dots represent average cumulative evaporative water loss from closed tubes from which plant stems and roots were removed. Error bars represent the standard deviation (n = 7-23; N = 2-3). n, number of biological replicates per genotype and condition; N, number of independent experiments.

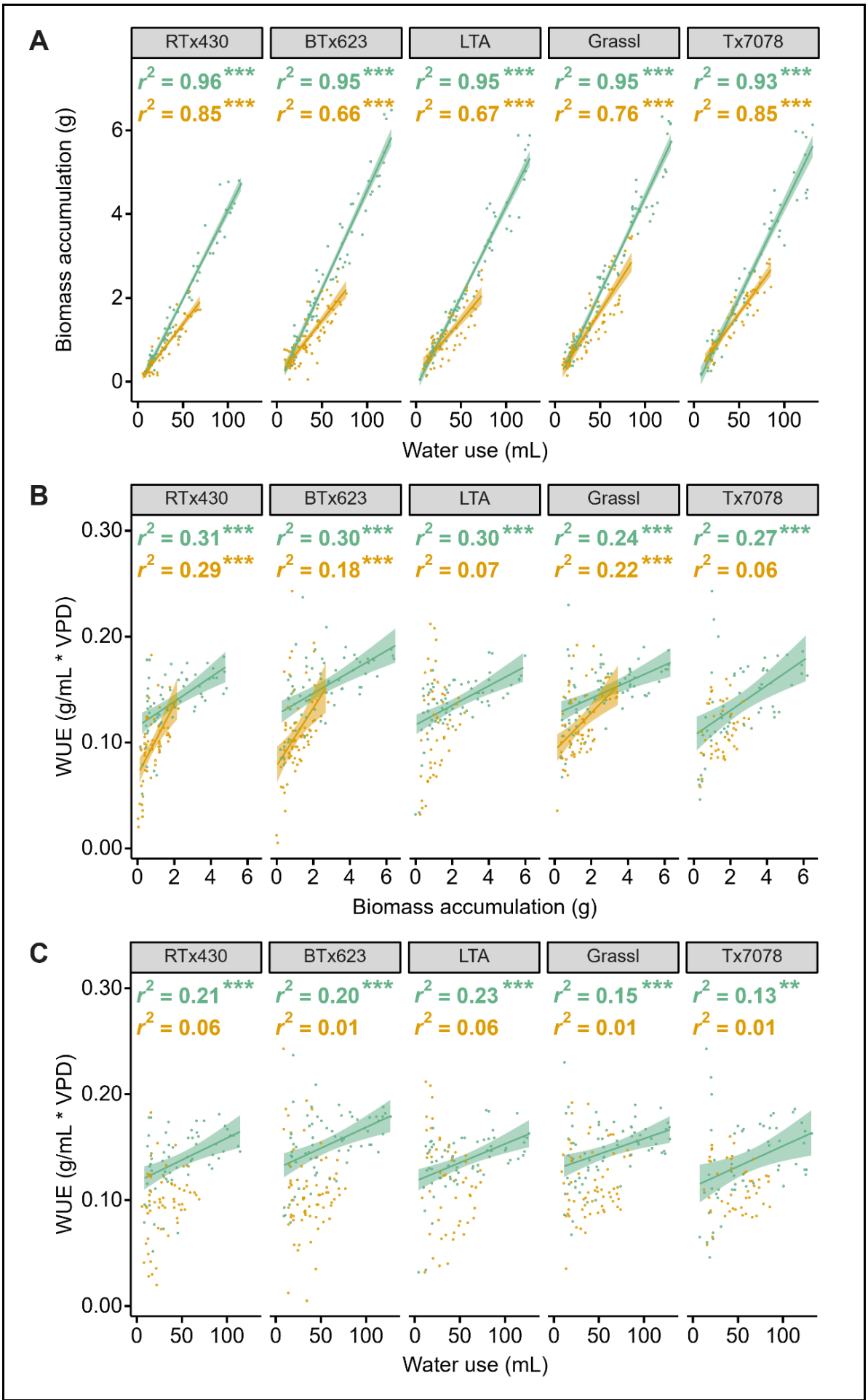
A
RTx430
BTx623
LTA
Grassl
Tx7078
r2 = 0.96***
r2 = 0.85***
r2 = 0.95***
r2 = 0.66***
r2 = 0.95***
r2 = 0.67***
r2 = 0.95***
r2 = 0.76***
r2 = 0.93***
r2 = 0.85***
Biomass accumulation (g)
Water use (mL)
B
r2 = 0.31***
r2 = 0.29***
r2 = 0.30***
r2 = 0.18***
r2 = 0.30***
r2 = 0.07
r2 = 0.24***
r2 = 0.22***
r2 = 0.27***
r2 = 0.06
WUE (g/mL * VPD)
Biomass accumulation (g)
C
r2 = 0.21***
r2 = 0.06
r2 = 0.20***
r2 = 0.01
r2 = 0.23***
r2 = 0.06
r2 = 0.15***
r2 = 0.01
r2 = 0.13**
r2 = 0.01
WUE (g/mL * VPD)
Water use (mL)

Figure S4: (A) Biomass accumulation as a function of water use, (B) WUE as a function of biomass accumulation, and (C) WUE as a function of water use in control (green) or mannitol-treated (orange) conditions. Solid lines represent the linear regression bounded by the 95% confidence interval (n = 12-18 per genotype, condition, and day; N = 4). r^2 values represent the square of the Pearson correlation coefficient of the linear regression. Asterisks indicate whether the linear relationship is statistically significant: ** (p-value < 0.01), *** (p-value < 0.001). Absence of a regression line indicates a non-significant linear relationship. n, number of biological replicates per genotype and condition; N, number of independent experiments.

Supplemental Tables

Table S1: 2-way ANOVA modelling the effect of genotype and time on delta-pH

Treatment	**Component**	**P-value**
Control	Genotype	0.388
	Days of measurement	< 2e-16
	Genotype*Days of measurement	0.090
Mannitol	Genotype	0.068
	Days of measurement	0.011
	Genotype*Days of measurement	0.203

Supplemental File 1: Initial pH, final pH, and delta-pH for all genotypes, conditions, and days of measurement.

Acknowledgements:

We thank I. Villa for help with drilling holes in both the ebb and flow system and all the screw-on caps, G. Materassi-Shultz for plant growth facility support, S. Mangat for help collecting data, members of the Rhee lab for helpful discussions, and the USDA National Plant Germplasm System for providing sorghum seeds. This work was done on the ancestral land of the Muwekma Ohlone Tribe, which was and continues to be of great importance to the Ohlone people.

Author contributions:

D.N.G. conceived of and designed the closed-hydroponic apparatus. D.N.G. and S.Y. R. conceived of the experimental design. D.N.G. and J.A.C. performed the growth experiments. J.A.C. and S.Y.R. provided intellectual contribution and input into manuscript organization. D.N.G. wrote the manuscript and S.Y.R. edited the manuscript. S.Y.R. advised D.N.G. and J.A.C.

Data availability:

All study data are included in the main text and supporting information.

Funding:

This project was funded in part by US National Science Foundation grants (MCB-1617020, IOS-1546838), Water and Life Interface Institute (WALII) DBI (grant no. 2213983), and US Department of Energy, Office of Science, Office of Biological and Environmental Research, Genomic Science Program grant nos. (DE-SC0018277, DE-SC0008769, DE-SC0020366, DE-SC0023160, and DE-SC0021286).

Conflict of interest:

The authors declare no conflict of interest.

References:

Ananda GKS, Myrans H, Norton SL, Gleadow R, Furtado A, Henry RJ. 2020. Wild Sorghum as a Promising Resource for Crop Improvement. Frontiers in Plant Science **11**.

Asao T (Ed.). 2012. *Hydroponics - A Standard Methodology for Plant Biological Researches*. InTech Open.

Balota M, Payne WA, Rooney W, Rosenow D. 2008. Gas Exchange and Transpiration Ratio in Sorghum. Crop Science **48**, 2361–2371.

Benjamin JG, Nielsen DC, Vigil MF, Mikha MM, Calderon F. 2014. Water Deficit Stress Effects on Corn (Zea mays, L.) Root:Shoot Ratio. Open Journal of Soil Science **4**, 151–160.

Boatwright JL, Brenton ZW, Boyles RE, *et al.* 2021. Genetic characterization of a Sorghum bicolor multiparent mapping population emphasizing carbon-partitioning dynamics. G3: Genes|Genomes|Genetics **11**, jkab060.

Bond BJ. 2000. Age-related changes in photosynthesis of woody plants. Trends in Plant Science **5**, 349–353.

Borrás L, Westgate ME, Astini JP, Echarte L. 2007. Coupling time to silking with plant growth rate in maize. Field Crops Research **102**, 73–85.

Butcher JD, Laubscher CP, Coetzee JC. 2017. A Study of Oxygenation Techniques and the Chlorophyll Responses of Pelargonium tomentosum Grown in Deep Water Culture Hydroponics. HortScience **52**, 952–957.

Cernusak LA, Aranda J, Marshall JD, Winter K. 2007. Large variation in whole-plant water-use efficiency among tropical tree species. New Phytologist **173**, 294–305.

Cha-um S, Kirdmanee C. Effect of osmotic stress on proline accumulation, photosynthetic abilities and growth of sugarcane plantlets (Saccharum officinarum L.). Pakistan Journal of Botany *in press*.

Chen W, Feng C, Guo W, Shi D, Yang C. 2011. Comparative effects of osmotic-, salt- and alkali stress on growth, photosynthesis, and osmotic adjustment of cotton plants. Photosynthetica **49**, 417–425.

Chenu K, Van Oosterom EJ, McLean G, *et al.* 2018. Integrating modelling and phenotyping approaches to identify and screen complex traits: transpiration efficiency in cereals. Journal of Experimental Botany **69**, 3181–3194.

Chochois V, Vogel JP, Rebetzke GJ, Watt M. 2015. Variation in Adult Plant Phenotypes and Partitioning among Seed and Stem-Borne Roots across Brachypodium distachyon Accessions to Exploit in Breeding Cereals for Well-Watered and Drought Environments. Plant Physiology **168**, 953–967.

Darko E, Végh B, Khalil R, Marček T, Szalai G, Pál M, Janda T. 2019. Metabolic responses of wheat seedlings to osmotic stress induced by various osmolytes under iso-osmotic conditions. PLOS ONE **14**, e0226151.

Dodd AN, Kusakina J, Hall A, Gould PD, Hanaoka M. 2014. The circadian regulation of photosynthesis. Photosynthesis Research **119**, 181–190.

Ehrenfeld JG, Ravit B, Elgersma K. 2005. Feedback in the Plant-Soil System. Annual Review of Environment and Resources **30**, 75–115.

Fageria NK, Baligar VC, Li YC. 2008. The Role of Nutrient Efficient Plants in Improving Crop Yields in the Twenty First Century. Journal of Plant Nutrition **31**, 1121–1157.

Fahlgren N, Feldman M, Gehan MA, *et al.* 2015. A Versatile Phenotyping System and Analytics Platform Reveals Diverse Temporal Responses to Water Availability in Setaria. Molecular Plant **8**, 1520–1535.

Falhof J, Pedersen JT, Fuglsang AT, Palmgren M. 2016. Plasma Membrane H+-ATPase Regulation in the Center of Plant Physiology. Molecular Plant **9**, 323–337.

Farquhar G, O'Leary M, Berry J. 1982. On the Relationship Between Carbon Isotope Discrimination and the Intercellular Carbon Dioxide Concentration in Leaves. Functional Plant Biology **9**, 121.

Fletcher A, Christopher J, Hunter M, Rebetzke G, Chenu K. 2018. A low-cost method to rapidly and accurately screen for transpiration efficiency in wheat. Plant Methods **14**, 77.

Foley JA, DeFries R, Asner GP, *et al.* 2005. Global Consequences of Land Use. Science **309**, 570–574.

Ge T, Sui F, Bai L, Tong C, Sun N. 2012. Effects of water stress on growth, biomass partitioning, and water-use efficiency in summer maize (Zea mays L.) throughout the growth cycle. Acta Physiologiae Plantarum **34**, 1043–1053.

Granier C, Vile D. 2014. Phenotyping and beyond: modelling the relationships between traits. Current Opinion in Plant Biology **18**, 96–102.

Grossiord C, Buckley TN, Cernusak LA, Novick KA, Poulter B, Siegwolf RTW, Sperry JS, McDowell NG. 2020. Plant responses to rising vapor pressure deficit. New Phytologist **226**, 1550–1566.

Großkinsky DK, Svensgaard J, Christensen S, Roitsch T. 2015. Plant phenomics and the need for physiological phenotyping across scales to narrow the genotype-to-phenotype knowledge gap. Journal of Experimental Botany **66**, 5429–5440.

Grzesiak MT, Grzesiak S, Skoczowski A. 2006. Changes of leaf water potential and gas exchange during and after drought in triticale and maize genotypes differing in drought tolerance. Photosynthetica **44**, 561–568.

Hanley ME, Fenner M, Whibley H, Darvill B. 2004. Early plant growth: identifying the end point of the seedling phase. New Phytologist **163**, 61–66.

Henderson S, Caemmerer SV, Farquhar GD, Wade L, Hammer G. 1998. Correlation between carbon isotope discrimination and transpiration efficiency in lines of the C4 species Sorghum bicolor in the glasshouse and the field. Functional Plant Biology **25**, 111.

Hubick K, Farquhar G, Shorter R. 1986. Correlation Between Water-Use Efficiency and Carbon Isotope Discrimination in Diverse Peanut (Arachis) Germplasm. Functional Plant Biology **13**, 803.

Kang S, Shi W, Zhang J. 2000. An improved water-use efficiency for maize grown under regulated deficit irrigation. Field Crops Research **67**, 207–214.

Kardol P, De Deyn GB, Laliberté E, Mariotte P, Hawkes CV. 2013. Biotic plant–soil feedbacks across temporal scales. Journal of Ecology **101**, 309–315.

Khalifa M, Eltahir EAB. 2023. Assessment of global sorghum production, tolerance, and climate risk. Frontiers in Sustainable Food Systems **7**.

Lambers H, Oliveira RS. 2019. Role in Ecosystem and Global Processes: Ecophysiological Controls. In: Lambers H, Oliveira RS, eds. Plant Physiological Ecology. Cham: Springer International Publishing, 677–698.

Leakey ADB, Ferguson JN, Pignon CP, Wu A, Jin Z, Hammer GL, Lobell DB. 2019. Water Use Efficiency as a Constraint and Target for Improving the Resilience and Productivity of C3 and C4 Crops. Annual Review of Plant Biology **70**, 781–808.

Lenth RV. 2016. Least-Squares Means: The R Package lsmeans. Journal of Statistical Software **69**, 1–33.

Li Z, Guo R, Li M, Chen Y, Li G. 2020. A review of computer vision technologies for plant phenotyping. Computers and Electronics in Agriculture **176**, 105672.

Liu D, Paul A-L, Morgan KT, Liu G. 2022. Effects of oxygen fertilization on damage reduction in flooded snap bean (Phaseolus vulgaris L.). Scientific Reports **12**, 4282.

Luo H, Zhao W, Wang Y, *et al.* 2016. SorGSD: a sorghum genome SNP database. Biotechnology for Biofuels **9**, 6.

Marschner H, Römheld V, Horst WJ, Martin P. 1986. Root-induced changes in the rhizosphere: Importance for the mineral nutrition of plants. Zeitschrift für Pflanzenernährung und Bodenkunde **149**, 441–456.

Medrano H, Tomás M, Martorell S, Flexas J, Hernández E, Rosselló J, Pou A, Escalona J-M, Bota J. 2015. From leaf to whole-plant water use efficiency (WUE) in complex canopies: Limitations of leaf WUE as a selection target. The Crop Journal **3**, 220–228.

Menz MA, Klein RR, Unruh NC, Rooney WL, Klein PE, Mullet JE. 2004. Genetic Diversity of Public Inbreds of Sorghum Determined by Mapped AFLP and SSR Markers. Crop Science **44**, 1236–1244.

Miller FR. 1984. Registration of RTx430 Sorghum Parental Line. Crop Science **24**, 1224–1224.

Mortlock MY, Hammer GL. 2000. Genotype and Water Limitation Effects on Transpiration Efficiency in Sorghum. Journal of Crop Production **2**, 265–286.

Murray FW. 1967. On the Computation of Saturation Vapor Pressure. Journal of Applied Meteorology and Climatology **6**, 203–204.

Narsai R, Rocha M, Geigenberger P, Whelan J, van Dongen JT. 2011. Comparative analysis between plant species of transcriptional and metabolic responses to hypoxia. New Phytologist **190**, 472–487.

Paine CET, Marthews TR, Vogt DR, Purves D, Rees M, Hector A, Turnbull LA. 2012. How to fit nonlinear plant growth models and calculate growth rates: an update for ecologists. Methods in Ecology and Evolution **3**, 245–256.

Panter SN, Jones DA. 2002. Age-related resistance to plant pathogens. Advances in Botanical Research. Academic Press, 251–280.

Pennisi BV, Thomas PA. *Essential pH Management in Greenhouse Crops*. University of Georgia.

Peters W, van der Velde IR, van Schaik E, *et al.* 2018. Increased water-use efficiency and reduced CO2 uptake by plants during droughts at a continental scale. Nature Geoscience **11**, 744–748.

Rascher U, Blossfeld S, Fiorani F, *et al.* 2011. Non-invasive approaches for phenotyping of enhanced performance traits in bean. Functional Plant Biology **38**, 968–983.

Reed DW (Ed.). 1996. *A grower's guide to water, media, and nutrition for greenhouse crops*. Batavia, Ill., USA: Ball Pub.

Rellán-Álvarez R, Lobet G, Lindner H, *et al.* 2015. GLO-Roots: an imaging platform enabling multidimensional characterization of soil-grown root systems. (MJ Harrison, Ed.). eLife **4**, e07597.

RESNIK ME. 1970. Effect of Mannitol and Polyethylene Glycol on Phosphorus Uptake by Maize Plants. Annals of Botany **34**, 497–504.

Ryan PR, Dessaux Y, Thomashow LS, Weller DM. 2009. Rhizosphere engineering and management for sustainable agriculture. Plant and Soil **321**, 363–383.

Shakoor N, Lee S, Mockler TC. 2017. High throughput phenotyping to accelerate crop breeding and monitoring of diseases in the field. Current Opinion in Plant Biology **38**, 184–192.

Shen J, Li C, Mi G, Li L, Yuan L, Jiang R, Zhang F. 2013. Maximizing root/rhizosphere efficiency to improve crop productivity and nutrient use efficiency in intensive agriculture of China. Journal of Experimental Botany **64**, 1181–1192.

Sinclair TR. 2012. Is transpiration efficiency a viable plant trait in breeding for crop improvement? Functional Plant Biology **39**, 359–365.

Sinclair TR, Rufty TW. 2012. Nitrogen and water resources commonly limit crop yield increases, not necessarily plant genetics. Global Food Security **1**, 94–98.

Sivakumar J, Prashanth JEP, Rajesh N, Reddy SM, Pinjari OB. 2020. Principal component analysis approach for comprehensive screening of salt stress-tolerant tomato germplasm at the seedling stage. Journal of Biosciences **45**, 141.

Slama I, Ghnaya T, Hessini K, Messedi D, Savouré A, Abdelly C. 2007. Comparative study of the effects of mannitol and PEG osmotic stress on growth and solute accumulation in Sesuvium portulacastrum. Environmental and Experimental Botany **61**, 10–17.

Sugiyama A, Bakker MG, Badri DV, Manter DK, Vivanco JM. 2013. Relationships between Arabidopsis genotype-specific biomass accumulation and associated soil microbial communities. Botany **91**, 123–126.

Vadez V, Kholova J, Medina S, Kakkera A, Anderberg H. 2014. Transpiration efficiency: new insights into an old story. Journal of Experimental Botany **65**, 6141–6153.

Williams BA, Grantham HS, Watson JEM, *et al.* 2020. Minimising the loss of biodiversity and ecosystem services in an intact landscape under risk of rapid agricultural development. Environmental Research Letters **15**, 014001.

Xie T, Su P. 2012. Canopy and leaf photosynthetic characteristics and water use efficiency of sweet sorghum under drought stress. Russian Journal of Plant Physiology **59**, 224–234.

Xin Z, Aiken R, Burke J. 2009. Genetic diversity of transpiration efficiency in sorghum. Field Crops Research **111**, 74–80.

Xin Z, Franks C, Payton P, Burke JJ. 2008. A simple method to determine transpiration efficiency in sorghum. Field Crops Research **107**, 180–183.

Xu W, Cui K, Xu A, Nie L, Huang J, Peng S. 2015. Drought stress condition increases root to shoot ratio via alteration of carbohydrate partitioning and enzymatic activity in rice seedlings. Acta Physiologiae Plantarum **37**, 9.

Zhao X, Wang W, Zhang F, Deng J, Li Z, Fu B. 2014. Comparative Metabolite Profiling of Two Rice Genotypes with Contrasting Salt Stress Tolerance at the Seedling Stage. PLOS ONE **9**, e108020.